Fundamentals of 180° Acquisition and Reconstruction in SPECT Imaging

R.L. Eisner, D.J. Nowak, R. Pettigrew, and W. Fajman

Department of Radiology; and Carlyle Fraser Heart Center of Emory University at Crawford W. Long Memorial Hospital, Department of Medicine, Emory University School of Medicine, Atlanta, Georgia; and General Electric Company Medical Systems Group, Milwaukee, Wisconsin

The accuracy of the reconstructed images obtained from a 180° SPECT acquisition is directly related to the effects of resolution and attenuation in the acquired projection data. Computer simulation studies show that the tomographic point spread functions and the quality of ^{201}Tl myocardial perfusion transaxial images depend upon the specific 180° arc used for reconstruction. Significant distortions are predicted in ^{201}Tl myocardial images reconstructed from both 180° and 360° scans; with signal to noise being significantly better for 180° scans. An anterior 180° scan with a starting angle between right lateral and 45° RAO in ^{201}Tl myocardial imaging is recommended. Reconstructed images acquired from 180° and 360° elliptical orbits are predicted to show more distortion than those obtained from circular acquisitions.

J Nucl Med 27:1717–1728, 1986

In the ideal situation, only 180° of view data is needed to obtain an accurate reconstructed image from a single photon emission computed tomographic (SPECT) acquisition. However, most technical studies in the literature have addressed the fundamentals of the tomographic reconstruction process related to 360° acquisitions (*1–3*). Most of these studies have employed the filtered backprojection algorithm, and use either the arithmetic or geometric mean of opposing 180° views in an attempt to average out the degrading effects of attenuation, scatter, and variable resolution. In cardiac studies with thallium-201 (^{201}Tl) these degrading factors for the 80 keV photon through the thorax are severe. For this and other specialized clinical applications 180° acquisition and reconstruction algorithms have been employed (*1,4–6*).

This paper describes the fundamental imaging considerations associated with 180° tomographic reconstruction using the filtered backprojection algorithm. The descriptions of the degrading effects are obtained through the use of computer simulated models. Where appropriate, data obtained from point source, phantom, and patient acquisitions are used to confirm and to further enhance the predictions of the models. In "Computer Simulations and Experimental Results for Point Source Reconstructions", the tomographic point spread function is determined for 180° arcs, with various starting angles, and the effects due to the variations of attenuation and resolution are presented. In "Cardiac (^{201}Tl Myocardial Perfusion) Imaging-Computer Simulation and Experimental Results for 180° Acquisition and Reconstruction", through the use of computer simulations, the effects of 180° acquisition and reconstructions on ^{201}Tl myocardial perfusion images is investigated and the results are compared with data obtained from patient studies. "Other Aspects of Cardiac Tomographic Analysis" is concerned with a study of various aspects of the reconstruction process related to important clinical considerations. Here, the simulation approach is used to compare the accuracy of the reconstructed ^{201}Tl myocardial perfusion images obtained for 360° and 180° circular acquisitions as well as from elliptical orbits. In addition, the degree of distortion and the nature of the reconstruction artifacts which result from center of rotation errors are discussed. The discussion summarizes the results with a focus on clinical application.

Received Dec. 10, 1985; revision accepted Apr. 4, 1986.

For reprints contact: R. L. Eisner, PhD, Director, Imaging Science Laboratory, Dept. of Radiology, Emory University School of Medicine, 412 Woodruff Memorial Building, Atlanta, GA 30322.

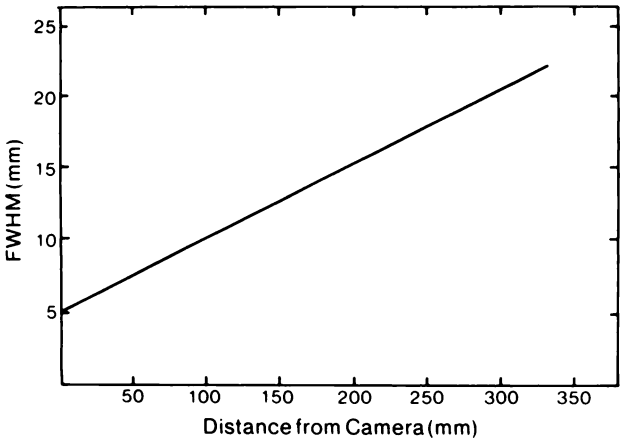

FIGURE 1
Resolution dependence (in air) on object distance from collimator surface for input into simulation program

COMPUTER SIMULATIONS AND EXPERIMENTAL RESULTS FOR POINT SOURCE RECONSTRUCTIONS

180° Acquisition-Resolution Effects

Computer simulation was used to isolate the effects of the view-to-view variation of the depth dependent resolution from the effects of attenuation on the tomographic point spread function. Resolution effects were investigated by the computer simulated imaging of a series of point sources located at various distances from a rotating camera system equipped with a low-energy, general-purpose collimator (LEGP). For each view the resolution variation with object depth from the camera system is described by the graph* shown in Fig. 1. Various 180° acquisitions and reconstructions were simulated with different initial starting angles, relative to the locations of the sources.

For these and all subsequent simulations noise-free planar views were calculated as projections from a mathematically defined transaxial slice image. This image was used to describe the distribution of radioactivity. The distribution of attenuation coefficients was generated in another image. The effects of resolution were incorporated into the projection data by convolving the attenuation modified activity data with a Gaussian MTF function whose full width at half maximum (FWHM) depended on the object to camera distance according to Fig. 1. For each view simulated projection data were acquired. The acquisition matrix size and the number of views acquired depended on the actual simulation. Data were filtered using a RAMP filter. Unless specifically stated, no attenuation correction was used. The effects of scatter were not included in the simulations.

Symmetric acquisition. In Fig. 2A the 180° acquisition which is symmetric about a line through the points is schematically described. The four point sources are located at distances of 5, 10, 15 and 20 cm from the camera surface in the closest view and the radius of rotation is 20 centimeters. The tomographic reconstruction of the points is shown in Fig. 2B. The tomographically derived point spread functions are elliptical with the minor axis of the ellipse lying parallel to the face of the collimator when the detector is in the view which has the best planar resolution. The minor axis of the ellipse is also in the direction of best tomographic resolution. Due to the nature of the tomographic reconstruction process the parameter of the point reconstruc-

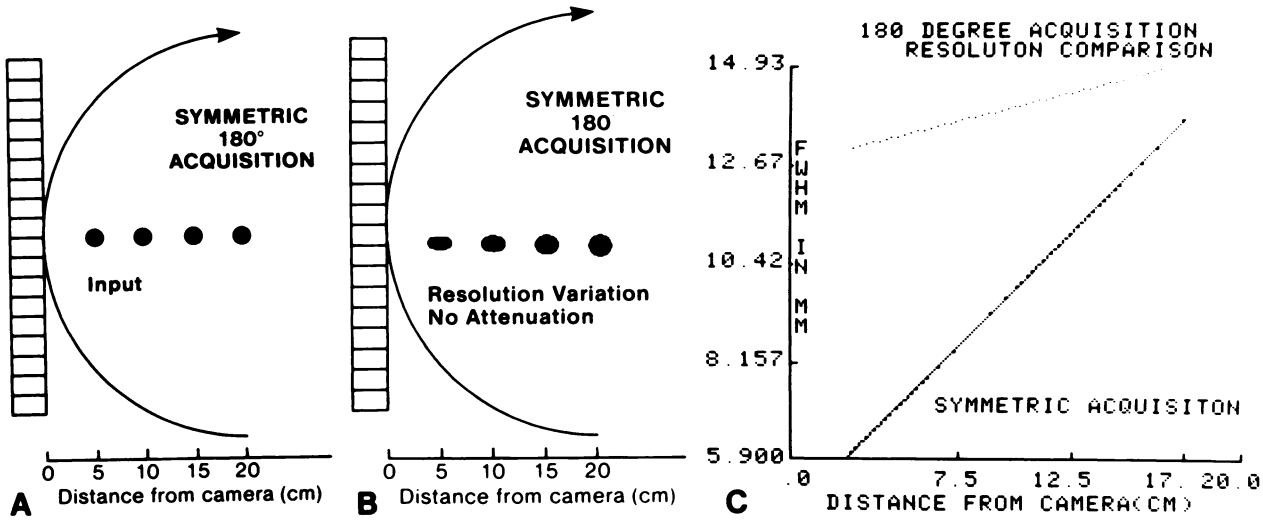

FIGURE 2
A: Schematic representation of 180° symmetric camera acquisition. B: Tomographic reconstructions of symmetrically acquired point sources. C: Tangential (solid curve) and radial (dotted curve) components of tomographic point spread functions

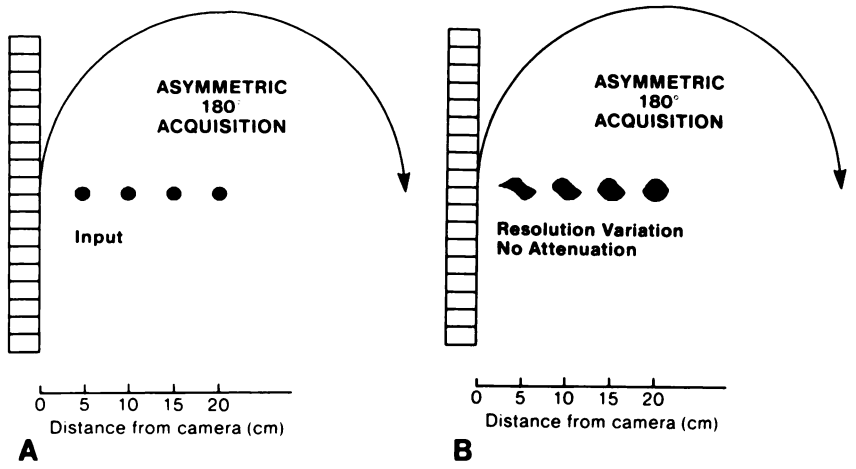

FIGURE 3
A: Schematic representation of 180° asymmetric acquisition. B: Tomographic reconstruction of asymmetrically acquired point sources

tions are best determined through a definition of the tangential and radial components of resolution. For the case presented here, the direction of the tangential component of resolution is that of the minor axis of the ellipse while the radial component lies along the major axis. The closest point (at 5 cm) shows the best tangential component of resolution. The 20-cm point which is at the center of rotation has a circular shape which is indicative of equal contributions from all the planar views in the reconstruction process with equal tangential and radial resolution components.

The values of the FWHM along the tangential and radial directions are shown in Fig. 2C as a function of the point source distance from the camera surface in the closest view. The solid and dotted curves describe the depth dependence of the tangential and radial component of resolution, respectively. The large differences between the two curves is indicative of the enhanced tangential resolution for points closest to the camera surface. At 20 cm distance from the camera surface the tangential and radial components of resolution are equal.

Asymmetric acquisition. Simulations were also performed for acquisitions asymmetric about the line through the points. The most asymmetric of these acquisitions is schematically described in Fig. 3A. Here, the camera starts acquiring data in the closest view and ends in the most distant view 180° away. Distortions of the point source reconstructions are evident in Fig. 3B. The shape of the point spread function is difficult to

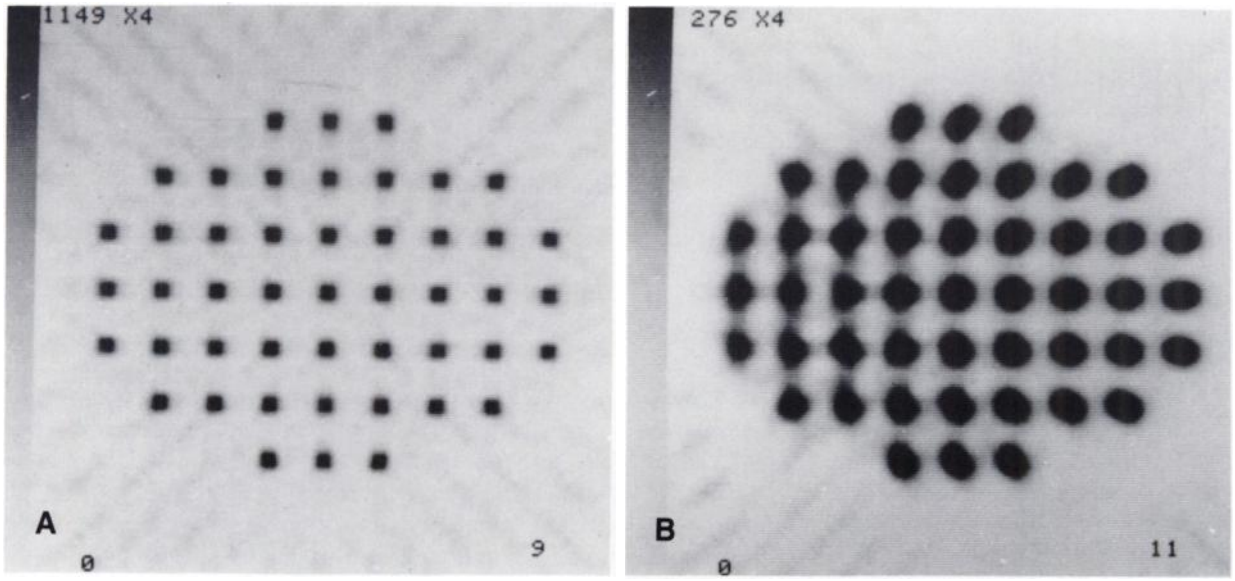

FIGURE 4
A: Simulated phantom of 2 pixel by 2 pixel point sources embedded in 60 pixel by 40 pixel elliptical medium. Acquisition is performed using 180° arc starting at top and ending in bottom position. Rotation is around right side of image. B: Results of tomographic reconstruction of phantom acquisition. Shape of point spread function depends on exact location of point with respect to camera arc

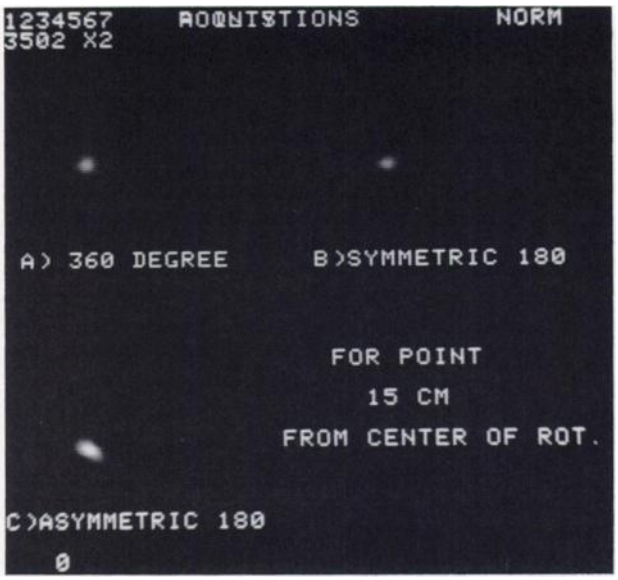

FIGURE 5
Comparison of point source reconstructions for object placed 15 cm from center of rotation. Radius of rotation of camera system is 20 cm

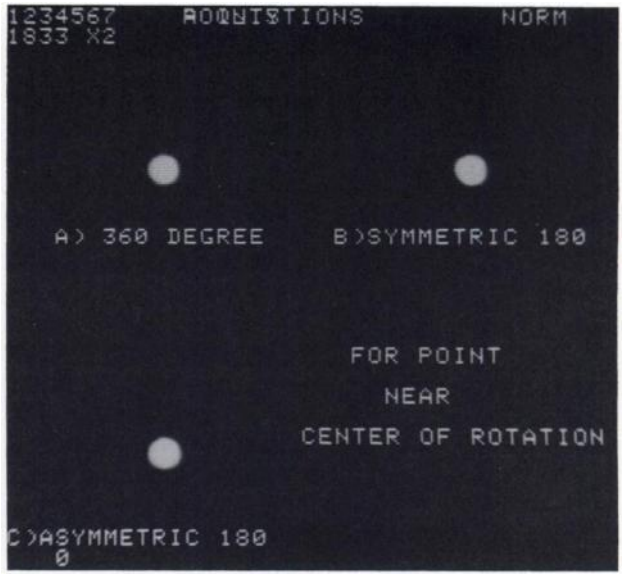

FIGURE 6
Comparison of point source reconstructions for object placed near center of rotation. Data are shown at different window and level as compared with Fig. 5 so that relative values of tangential and radial components of resolution are not easily compared in the two figures

describe; however, the main feature is that the point spread functions are very different from those of the symmetrically acquired point source reconstructions. This is further illustrated in Fig. 4 where the tomographic reconstruction of (1.2 cm × 1.2 cm) point sources embedded in a simulated elliptical phantom is shown. The acquisition was symmetric about the major axis of the phantom and the 180° arc was about the right side of the image. The points along the center line of the phantom show the elliptical point spread functions. Point reconstructions become more circular near the center of the phantom (i.e., near the center of rotation). The direction of best resolution changes for points located on the far side of the center of rotation with radial resolution better than tangential resolution the further the point is located from the center of rotation. For asymmetric data acquisition the point source reconstructions have distorted elliptical shapes with best resolution in a direction which is approximately parallel to the camera surface for those views in which the point was imaged with the best planar resolution.

Experimental results-point source reconstructions. To test the predictions of the computer simulations experimental data were acquired of a ^{99m}Tc point source placed in positions corresponding to those used in the isolated point source simulation program described above. Data were acquired at a fixed radius of rotation of 20 cm with 64 views over 360° and into a 64 × 64 acquisition matrix. Data were then reconstructed over 180° arcs with various starting angles.

The point source reconstructions of the ^{99m}Tc point placed 15 cm from the center of rotation are shown in Fig. 5 for the symmetric 180°, the asymmetric 180° and the 360° acquisition. In Fig. 6 the corresponding reconstructions are shown for the point source located near the center of rotation.

In agreement with prediction:

1. The point spread function for a symmetrically acquired point is elliptical with the tangential component of resolution better than the radial component of resolution. The tangential component of resolution is also better than that from the 360° reconstruction (cf. Fig. 5A and Fig. 5B) which also exhibits an elliptical point spread function (*7*).

2. The point spread function for an asymmetrically acquired point (Fig. 5C) is distorted from the elliptical shape, but generally has a minor axis which lies parallel to the face of the collimator in the view which had best planar resolution.

3. The point spread function for a point located near the center of rotation is circular (Fig. 6).

Attenuation Effects

To study the effect of variable attenuation with view direction on reconstructed image quality, computer simulations were performed with four [1.2 cm × 1.2 cm (2 pixel × 2 pixel)] test objects symmetrically placed inside a circular uniform attenuating medium ($\mu = 0.15$ cm^{-1}) with a radius of 12 cm (Fig. 7A). To simulate various types of clinical situations 180° data were acquired with the following distributions of simulated radioactivity inside the phantom: (a) radioactive objects in nonradioactive medium, (b) nonradioactive objects

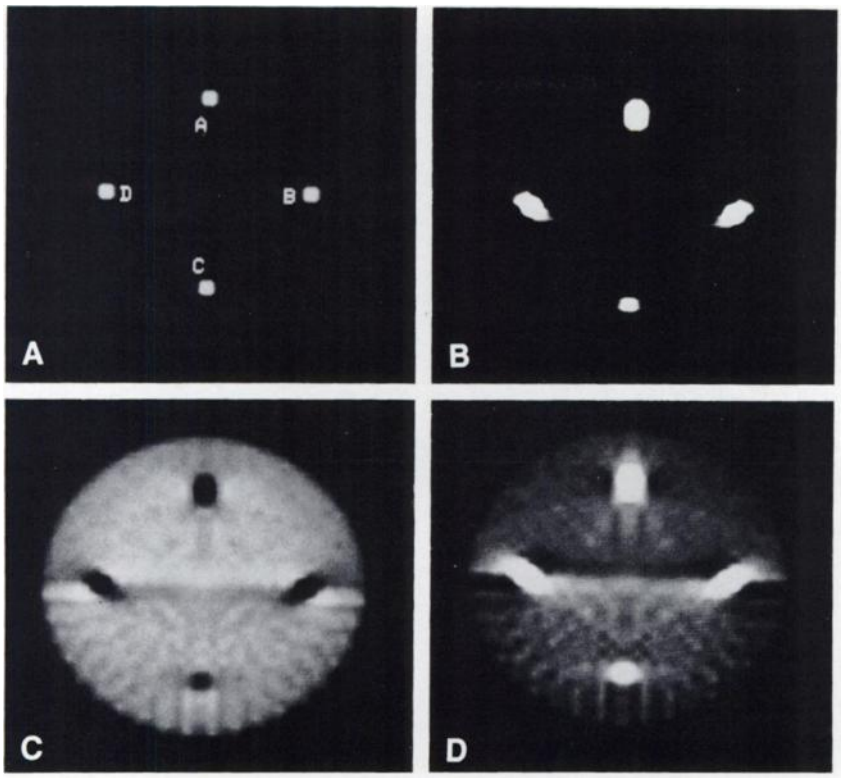

FIGURE 7
A: Simulated phantom of 2 pixel by 2 pixel rods embedded in circular attenuating medium ($\mu = 0.15$ cm^{-1}) with radius of 20 pixels. Rods are placed 12 pixels from center of phantom. B: Reconstruction of radioactive rods with no activity in surrounding. C: Reconstruction of voids with background activity. D: Reconstruction of radioactive rods with background activity. Distortions of rods is apparent with streaking artifact present between rods B and D

(voids) in radioactive medium, and (c) radioactive objects in radioactive background.

All reconstructions were from 32 views over the anterior portion of the phantom (i.e., symmetric about point A in Fig. 7A). The tomographic reconstruction used a RAMP filter and for Cases 2 and 3, as might be done clinically, a simple preprocessing (*8*) attenuation correction was applied to the data. The resulting tomographic reconstructions are shown in Figs. 7B through 7D.

Figure 7B (type 1) exhibits distortions similar to those found with variable view resolution. Points B and D which are asymmetrically acquired have a distorted elliptical shape with minor axis approximately parallel to the camera face in that view which had minimum attenuation effects. The reconstructed shape of point A, which was symmetrically acquired, is elliptical while point C which is always at the greatest distance from the camera surface shows a marked decrease in reconstructed counts.

In Fig. 7C (type 2) the shapes of the reconstructed voids are similar to those of the radioactive rods shown in Fig. 7B. The contrast of the voids depends on their exact position inside the phantom. A large streaking artifact passes between points B and D.

In Fig. 7D (type 3) the shapes of the reconstructed radioactive rods are as in type 1. The large streaking artifact between points B and D is reversed in magnitude when compared with type 2.

Thus, asymmetric attenuation effects are predicted to distort object shape and produce streak artifacts in 180° reconstructed tomographic images.

CARDIAC (^{201}TL MYOCARDIAL PERFUSION) IMAGING-COMPUTER SIMULATION AND EXPERIMENTAL RESULTS FOR 180° ACQUISITION AND RECONSTRUCTION

Much of the clinical experience with 180° tomographic acquisition has been with ^{201}Tl myocardial perfusion imaging. Our simulation study is now directed to an investigation of the effects of attenuation and resolution on the quality of the reconstructed cardiac tomograph.

Resolution Effects: Symmetric Acquisition

The effect of spatial resolution variation with object distance from the collimator surface on the reconstruction of radioactivity which was distributed uniformly in the walls of the myocardium was initially investigated. A slice of the cardiac wall simulated as a semicircular annulus with constant activity is shown in Fig. 8A. Two 180° acquisitions each symmetric about the apex of the phantom were simulated. The apex was at 0 cm and 15 cm from the center of rotation and the radius of rotation was 20 cm. The data were reconstructed using a Ramp filter. The reconstructed images as well as a maximal count circumferential profile around the half-annulus are shown in Figs. 8B and 8C for the 15 cm and 0 cm acquisitions, respectively. For

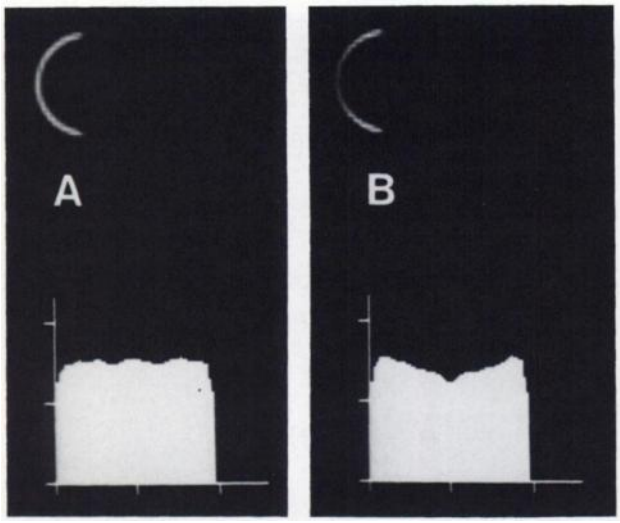

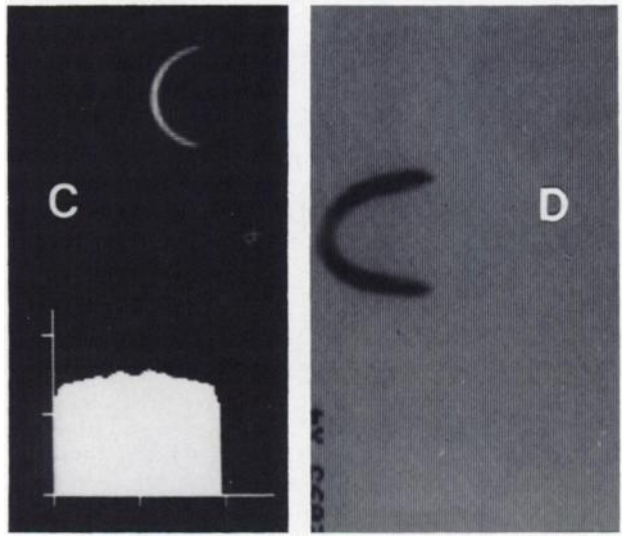

FIGURE 8
Effect of camera-collimator resolution on myocardial phantom reconstruction with 180° acquisition. A: Reconstruction of computer simulated half annulus placed 15 cm from center of rotation. Camera rotation around left side of phantom is symmetric about apex. Effects of resolution have not been included. B: As for Fig. 8A, but effects of resolution have been included. Count density decrease occurs in apical region. C: As for Fig. 8B, but apex of phantom is placed at center of rotation. Increase in count density occurs in apical region. D: Reconstruction of ^{99m}Tc filled polyethylene tubing placed ~15 cm from center of rotation. As in computer simulation decrease in count density is observed in apical region

the reconstructions in which the apex is located 15 cm from the center of rotation the apical region shows a decrease or an apparent defect in maximal counts. We find that as the simulated myocardium is moved towards the center of rotation the apical defect diminishes in intensity. When the apex sits on the center of rotation (Fig. 8C) the apical area shows an increase in maximal counts as compared to its neighboring walls. The apical defect is a reflection of the fact that in the tomographic

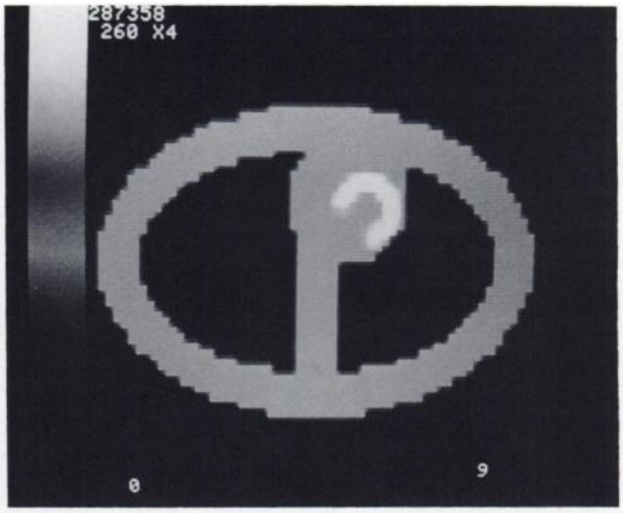

FIGURE 9
Simulated thorax phantom shows myocardium embedded in attenuating medium which includes chest wall, heart, backbone and lungs

backprojection process the edge resolution at the apex is determined primarily by the laterally acquired views; the resolution of the walls adjacent to the apex is determined by the closer, more anterior views, which have relatively better resolution. This resolution difference causes an observed broadening of the wall and a corresponding decrease in count density in the apical region as shown in Fig. 8B. In contrast, when the apex sits on the center of rotation the camera is closer in the lateral views than in the anterior views so that the reconstruction process provides a better resolved apical wall compared to the regions adjacent to it. This effect produces the observed relative increase in count density in the apical region shown in Fig. 8C.

Resolution Effects: Experimental Results

To confirm this observation a phantom was constructed which consisted of a polyethylene tubing filled with technetium-99m (^{99m}Tc) and bent to form a semicircular annulus and placed ~15 cm from the center of rotation. Data were acquired symmetrically about the apex and reconstructed as in the simulation. As shown in Fig. 8D, and in agreement with prediction, the apex of the reconstructed tube shows a relative decrease in count density when compared to the adjacent walls. When the apex of the tube was placed at the center of rotation a corresponding increase in count density was observed (not shown). Thus, the resolution effects play an important role in determining the degree of count density distortion in the reconstructed tomographic image.

Cardiac (^{201}Tl) Simulations: Resolution and Attenuation Effects

Description of myocardial phantom. To better simu-

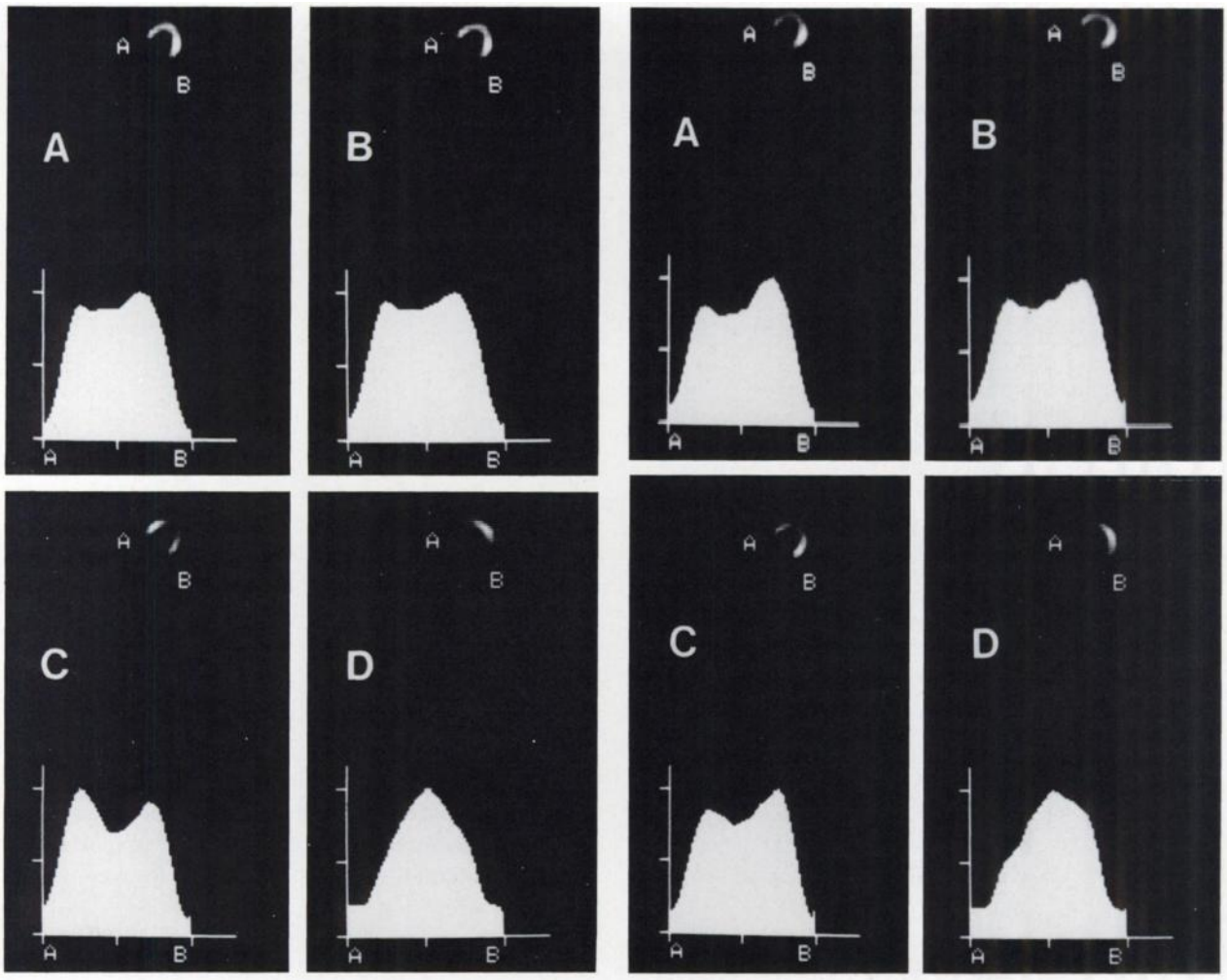

FIGURE 10
180° tomographic reconstruction for myocardium embedded in constant attenuator. Maximal count circumferential profile analysis starts on septal wall (side A) and ends on lateral wall (side B). A: Left lateral to right lateral anterior acquisition. B: Anterior 45° RAO to LPO acquisition. C: Anterior to posterior 180° acquisition (around left side). D: Posterior 45° RAO to LPO acquisition (opposite to that in Fig. 10B). For optimal display each image has been independently normalized, so that relative counts for different acquisitions cannot be determined from these images

FIGURE 11
Tomographic reconstruction of myocardium embedded in thorax attenuator. A: Left lateral to right lateral anterior acquisition. B: Anterior 45° RAO to LPO acquisition. C: Anterior to posterior acquisition, around left side. D: Posterior 45° RAO to LPO acquisition (opposite to that in Fig. 11B)

late the heart wall inside the body a computer model was developed for a two-dimensional myocardium. The heart shape was modeled as three-quarters of an annulus with heart wall thickness of 1.2 cm. This cardiac phantom was placed inside an elliptical body phantom with a major axis of 36 cm and minor axis of 24 cm. To qualitatively study the range of effects possible in clinical situations, the interior of the elliptical phantom was filled with either a uniform attenuator (μ = 0.18 cm^{-1}) or was chosen to mimic the attenuation due to the main structures inside the thorax. In the latter case, since we are only interested in investigating the major effects of attenuation on image quality, we have assigned to all structures other than the lungs the same attenuation coefficient (μ = 0.18 cm^{-1}). For the lungs the value μ = 0.06 cm^{-1} was used. These values (*1*) represent reasonable choices for use with the structures and photon energies of interest. In particular, the simulations should provide a simple but reasonable model for ^{201}Tl as well as for ^{99m}Tc myocardial imaging. The myocardial apex was directed along the 45° LAO direction and was placed 1.2 cm from the inside of the chest wall which was 3.6 cm thick. This simulated phantom is shown in Fig. 9, where the simulated heart wall is shown in white and the thorax attenuation model is shown in gray.

Acquisition/reconstruction. Various simulated acquisitions using the resolution variation with distance of the LEGP collimator were performed and included:

1. Circular acquisition with 18.5 cm radius of rota-

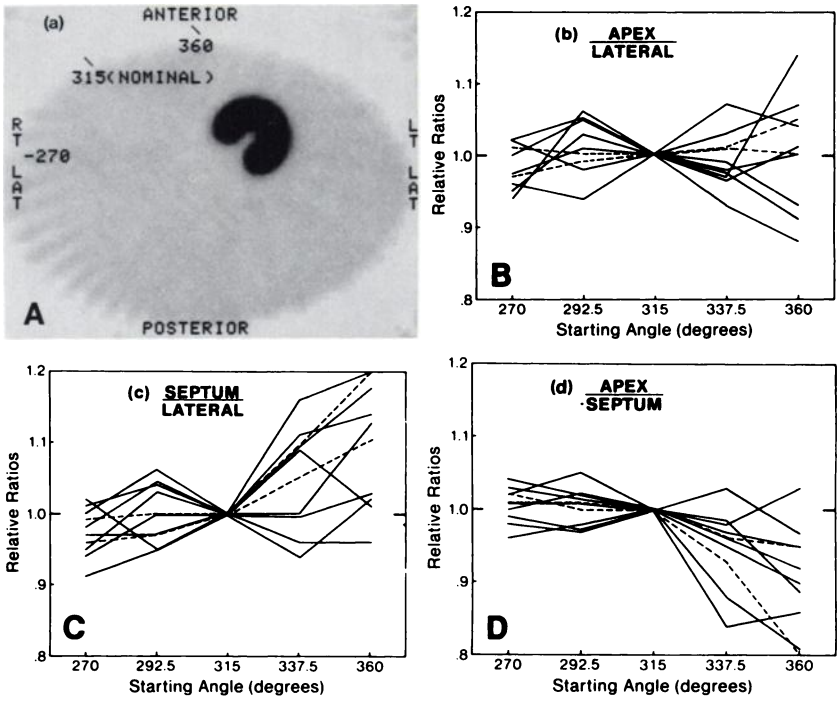

FIGURE 12
A: View (standard CT orientation) of myocardium embedded in elliptical body phantom. Starting angles correspond to those shown in Figs. 12B through 12D. B: Relative ratio of apex to lateral wall with respect to corresponding ratio at 45° RAO (315°) starting angle. C: As in Fig. 12B, but for septum/lateral wall ratio. D: As in Fig. 12C, but for apex/septal wall. Solid curves are from data obtained from clinical ^{201}Tl studies. Dotted lines in figures are corresponding ratios for models described in text

tion with various 180° arcs. The value of the radius of rotation is consistent with that used in clinical acquisitions. The camera is 0.5 cm from the phantom in the lateral views. In all other views it is further away.

2. Circular acquisition with 18.5 cm radius of rotation with a 360° rotation.

3. Elliptical acquisition with a major axis of 37 cm (i.e., equal to the diameter of the circular acquisition) and minor axis of 25 cm with various 180° arcs. As might be done in a clinical acquisition, the major and minor axis of the ellipse were chosen so that the rotating camera-collimator path was almost touching (within 0.5 cm) the elliptical body outline of the simulated phantom in all views.

All data were simulated as if acquired in 64 views over 360° and filtered backprojection was performed using a Ramp filter. The reconstructed counts in the myocardial slice were quantified through the use of a maximum count circumferential profile analysis.

Results of cardiac (^{201}Tl) simulations: Effects of attenuation and resolution on reconstructed tomograms for various circular 180° acquisitions. Tomographic slices were reconstructed for the following 180° acquisition arcs: (a) left lateral to right lateral around the anterior; (b) 45° RAO to LPO around left side-nominal acquisition; (c) anterior to posterior around left side; (d) 45° RAO to LPO around right side (which represents data taken from the opposite 180° segment to that in case b).

Reconstructed images are shown in Fig. 10 and in Fig. 11 for the cases of uniform attenuator and modeled thorax attenuator, respectively. From these figures it is apparent that for all acquisition arcs, the effects of variable attenuation and resolution are to distort the reconstructed tomograms from their input constant density. Moreover, measures of the distortion, the septal to lateral wall ratio or the degree of the apical defect are dependent on the exact 180° arc used for reconstruction.

Comparison with patient data: Thallium-201 myocardial perfusion images. To further quantify the extent of the effect of various 180° acquisition arcs, data from ^{201}Tl myocardial perfusion studies were investigated. The data were obtained from studies on eight subjects who were injected with 2.5 mCi of ^{201}Tl at peak exercise. Following an initial stress scan delayed images were obtained ~4 hr later with a rotating single headed gamma camera interfaced to a computer system†. Only the delay data were used in this study. They were acquired with a 64 view, 360° scan with the camera stopping for 30 sec at each view. Data were processed through the manufacturer's reconstruction program† using a Ramp-Hanning filter which was made to pass through zero at half the sampling frequency (0.833 cycles/cm). To realize a three dimensionally symmetric point spread function the view projection data were filtered with a [1 2 1] kernel along the axial directon. From the transaxials, oblique angle slices were obtained along the three mutually perpendicular planes in a coordinate system fixed to the heart. Three 6-mm-thick horizontal long axis slices were added together. These summed slices were subjected to a maximal count circumferential profile analysis. Counts were then summed over adjacent 45° wedges which subtended the apex and the anterior aspect of the septal and lateral wall. From these counts the following ratios were deter-

mined: (a) apex/lateral wall; (b) septal/lateral wall; and (c) apex/septal wall for anterior arc acquisitions with six different starting angles (see Fig. 12A for angular definitions). As an aid in qualitatively appreciating the change in ratio with view angle the relative ratios have been normalized to that at the nominal 45° RAO or 315°, starting angle. In Figs. 12B through 12D the relative ratio of the uptake in the walls of the myocardium are shown normalized to that obtained with the 45° RAO starting angle. No attempt has been made to take into account the actual angularity of each subject's heart with respect to the starting angle. The corresponding ratios derived from the myocardial simulations are shown as the dotted lines in the figures.

We see from Fig. 12 that the simulation studies qualitatively describe the dependence of the ratios with view angle. More importantly from a clinical perspective is that attenuation and resolution effects cause the relative ratio of the reconstructed ^{201}Tl uptake in the walls of the myocardium to depend on the exact 180° arc used for acquisition and reconstruction. The data in Fig. 12 show that the ratios are relatively insensitive to starting angles between 270° and 315°. As the starting view angle becomes more anterior the ratios begin to significantly deviate from their nominal values.

OTHER ASPECTS OF CARDIAC TOMOGRAPHIC ANALYSIS

Results of Cardiac (^{201}Tl) Simulations—Comparison of Circular 180° and 360° Acquisitions

There has been some controversy over the optimum scanning procedure for ^{201}Tl tomographic acquisitions. Most authors (*1,4–6*) have favored a 180° arc, but others (*9–11*) have argued for a 360° rotation. In Fig. 13, the results from uniform and thorax simulations for the 360° acquisitions (Fig. 13B and 13D) are compared with those for the nominal 45° RAO scans (Fig. 13A and 13C). In each attenuation case, for neither the nominal 180° acquisition nor the 360° acquisition does the output image provide a correct representation of the expected constant density of radioactivity in the heart wall. The low level artifacts for the thorax attenuator reconstruction are shown in Figs. 13E and 13F which are Figs. 13C and 13D but with a logarithmic gray scale map. The streaking artifacts are observed to be at similar levels of contrast in both the 180°-nominal and 360° images. For both the uniform and thorax attenuation model the data reconstructed from the backward (posterior) 180° segment (see Figs. 10D and 11D) which are included in the 360° reconstruction show significantly more distortion than does the nominal 180° tomogram. There is a large decrease in reconstructed counts in the septal and lateral wall regions in the backward data.

Thus, the model predictions show comparable distortions, and give no support for preference of a 360°

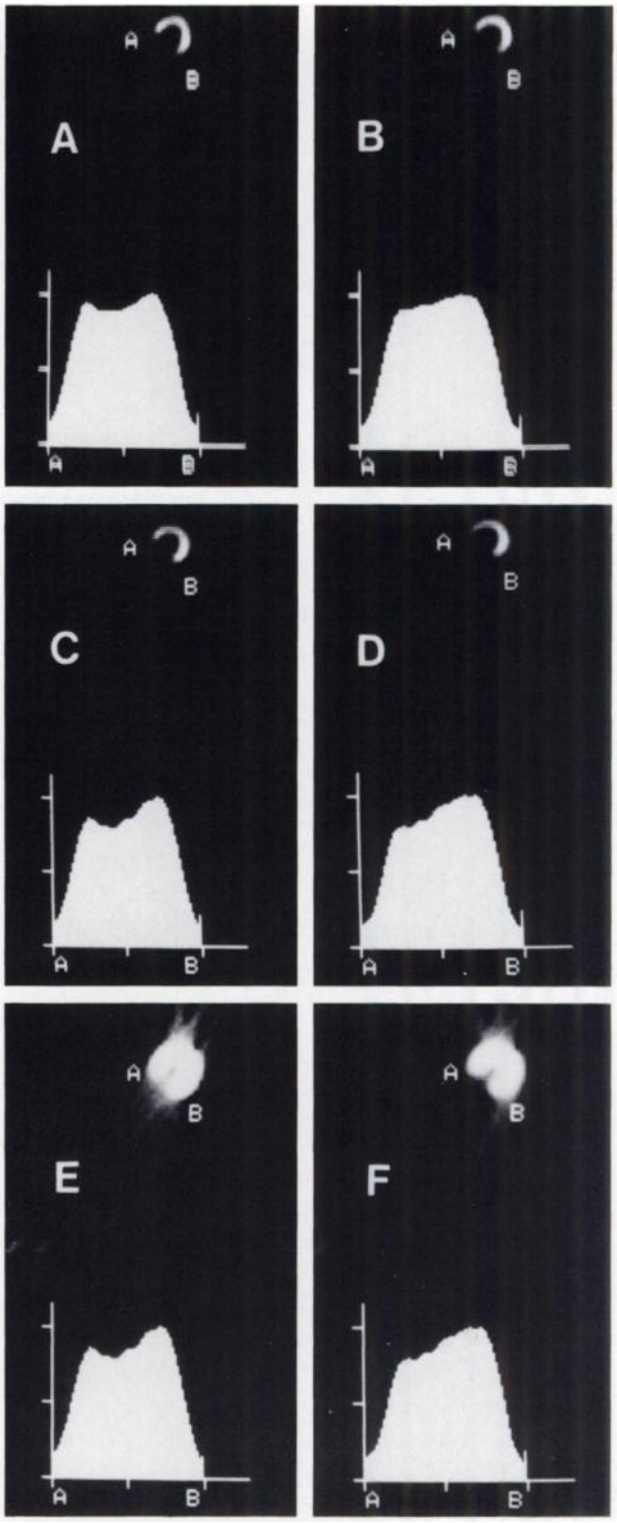

FIGURE 13
Comparison of tomographic reconstruction for nominal 180° and 360° acquisitions. A: Constant attenuator: 180° scan. B: Constant attenuator: 360° scan. C: Thorax attenuator: 180° scan. D: Thorax attenuator: 360° scan. To compare low level streak artifact generation, logarithmic map is employed. E: Thorax attenuator: 180° scan. F: Thorax attenuator: 360° scan. Distortions of approximately same significance are present in both 180° and 360° scans

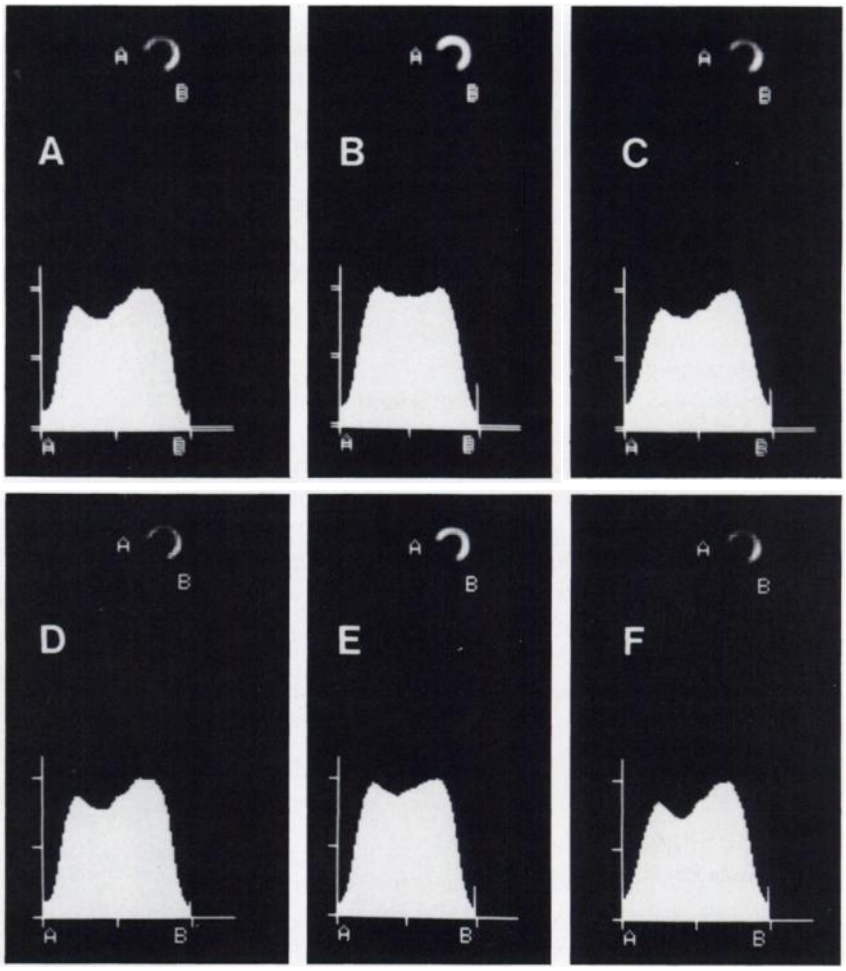

FIGURE 14
Comparison of circular and elliptical rotations-thorax attenuator model. A: Circular orbit: Attenuation effect only. B: Circular orbit: Resolution effect only. C: Circular orbit: Both attenuation and resolution effects. D: Elliptical orbit: Attenuation effect only. E: Elliptical orbit: Resolution effect only. F: Elliptical orbit: Both attenuation and resolution effects. Distortions are larger in elliptical orbit reconstruction (Fig. 14F) as compared with that of circular orbit reconstruction (Fig. 14C)

over a 180° acquisition as has been suggested (*9–11*). Moreover, for fixed patient acquisition times, significantly more cardiac counts (*1,6*) are obtained with a nominal 45° RAO 180° acquisition. Therefore, simple signal to noise considerations as well as the improved contrast resolution (*6*) would appear to strongly favor the 180° over the 360° ^{201}Tl acquisition.

Results of Cardiac Simulation: Comparison of Elliptical and Circular 180° Acquisitions

Many of the major camera/computer manufacturers now provide the capability to rotate the gamma camera in not only a circular but also an elliptical orbit about the patient. It is therefore of interest to compare the results from simulations using the two types of acquisition schemes. The camera is always closer to the subject being scanned for the elliptical orbit so that the resolution of the planar images is better than that of the circular scan; however, there is a larger relative difference between the resolution in the anterior and lateral views. The attenuation effects in the planar images are only determined by the structure of the phantoms and are identical for the data obtained from the two types of acquisitions. Figure 14 shows the cardiac reconstructions for circular (top) and elliptical (bottom) acquisitions for the simulated myocardium embedded in the thorax attenuation model. In each case, data were acquired over a 180° anterior arc starting at the nominal 45° RAO position. The reconstructed images shown in Fig. 14 isolate the effects of depth dependent resolution (Fig. 14B and 14E) and attenuation (Fig. 14A and 14D). The greater differences in planar resolution in the elliptical acquisition causes a correspondingly greater distortion of the count density in the walls of the myocardium in the resolution images. A comparison of Figs. 14C (circular) and 14F (elliptical) which have combined effects of resolution and attenuation shows that the resulting distortions (as measured by the relative wall ratios) due to resolution effects significantly affect the tomographic reconstruction even in the presence of effects due to attenuation.

Whereas, the results presented here should only be viewed as qualitative predictors of possible differences in the reconstructed tomograms they do suggest that normal values obtained from circular acquisitions and used to compare to reconstructed ^{201}Tl patient data may not be appropriate for data obtained from the corresponding elliptical scans.

Center of Rotation Errors-Effects on Cardiac Reconstructions

The effect of center of rotation errors on point source reconstructions has been well quantified and described (*12*). For a point source acquired with a 180° rotation, and with an error in the value of the center of rotation a tuning fork artifact distortion is present in the reconstructed slice. For a 360° acquisition, the same center of rotation error produces a broadening of the point source with no other apparent distortions. However, for large center of rotation errors the shape of the 360° point source reconstructions is that of an annulus.

An example of the effects of center of rotation error on cardiac reconstructions is shown in Fig. 15. The images were reconstructed following a plus or minus one pixel out of 64 error in the value of the center of rotation for simulated acquisitions of the cardiac phantom (constant density myocardium; no resolution degradation, no attenuation effects). Figures 15A and 15C which correspond to the 180° scan show marked distortion in the reconstructed count density with the defect and focal hot spot positions dependent on the sign of the center of rotation error. The 360° scans show no such distortions; however, there is a general broadening of the myocardium, an artifact which could potentially blur out defects actually present in the cardiac wall. Thus, rigid quality control procedures are necessary to ensure that an accurate value of the center of rotation is input into the tomographic reconstruction program. As seen in Fig. 15, an incorrect value can cause distortions in the ^{201}Tl reconstructed images.

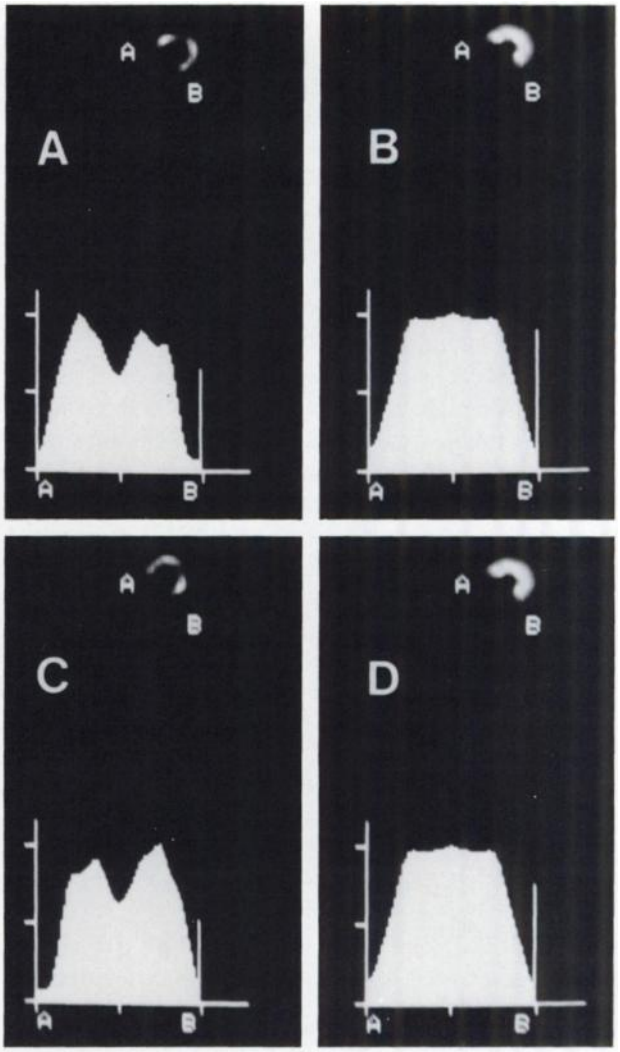

FIGURE 15
Effects of error in value of center of rotation on tomographic reconstruction. Correct value for center of rotation is 32.5. A: 180° acquisition: Center of rotation is assumed to be 31.5. B: 360° acquisition: Center of rotation is assumed to be 31.5. C: 180° acquisition: Center of rotation is assumed to be 33.5. D: 360° acquisition: Center of rotation is assumed to be 33.5. Reconstruction from 180° acquisition show marked distortion in reconstructed count density. Reconstructions from 360° acquisition show severe broadening of the myocardial wall

DISCUSSION

Tomographic reconstructions of 180° point source acquisitions which include attenuation and resolution effects show marked distortions. This is particularly apparent for data obtained from asymmetric acquisitions. The tomograms not only exhibit shape distortion, but as in the case of radioactive objects immersed in an attenuating medium other artifacts such as streaking patterns are present in the reconstructed images. Such features could have an adverse effect on diagnostic image interpretation. This has been observed clinically in [^{99m}Tc]pyrophosphate infarct-avid tomographic 180° scans (*13*). Thus, to reduce artifact generation most clinical studies should be acquired with 360° acquisitions; however, there would still be degradation of image quality caused by the poor data obtained in the views most distant from the reconstructed object. To significantly improve both spatial and contrast resolution in tomograms derived from 360° scans we have previously proposed (*14*) a new tomographic reconstruction technique, distance weighted filtered backprojection, which gives greater weight in the reconstruction process to the nearest of the 180° opposed views.

For the special case of ^{201}Tl myocardial imaging, the 180° acquisition is strongly favored over the 360° scan, since

1. There is improved resolution leading to improved contrast (*6*).
2. For fixed acquisition time (*1,6*) significantly more cardiac counts are acquired.
3. The posterior 180° data which is added to the forward 180° data to make the 360° tomogram is of exceptionally poor quality.
4. In either case, 180° or 360°, distortions are predicted to occur in the reconstructed tomograms. Even

if a 180° acquisition is chosen, the distortions caused by attenuation and resolution must be addressed to obtain maximum clinical diagnostic accuracy from the ^{201}Tl tomographic procedure. In lieu of adequate attenuation and resolution correction, which appears to be still unattainable, the best approach is to compare patient data with that obtained from matched normal subjects (*15–17*). Our studies suggest that, to avoid acquisition dependent effects, data should be acquired using an anterior 180° arc with starting angles between 270° (right lateral) and 315° (45° RAO).

The computer simulation models have been used as tools to isolate the effects of attenuation and resolution on tomographic image quality. The models are simple, but aid in relating effects seen in patient studies to the appropriate acquisition and reconstruction parameters. No attempt is made to use the results as quantitative predictors of clinical results, but they provide insight into the interplay between the acquisition and reconstruction parameters and the artifacts and distortions observed in clinical SPECT images.

FOOTNOTES

* General Electric, Milwaukee, WI (General Electric LEGP collimator).

† General Electric, Milwaukee, WI (General Electric 400AT/STAR).

REFERENCES

1. Larsson SA: Gamma camera emission tomography. *Acta Radiologica Suppl* 363, 1980
2. Jaszczak RJ, Murphy PH, Huard D, et al: Radionuclide emission computed tomography of the head with Tc-99m and a scintillation camera. *J Nucl Med* 18:373–380, 1977
3. Keyes JW, Orlandea N, Heetderks WJ, et al: The Humongotron-A scintillation camera transaxial tomograph. *J Nucl Med* 18:381–387, 1977
4. Ritchie JL, Olson DO, Williams DL, et al: Transaxial computed tomography with Tl-201 in patients with prior myocardial infarction. *J Nucl Med* 22:P11, 1981(abstr)
5. Besozzi MC, Rizzi HR, Rogers WL, et al: Rotating gamma camera ECT of Tl-201 in the human heart. *J Nucl Med* 22:P11, 1981(abstr)
6. Tamaki N, Mukai T, Ishii Y, et al: Comparative study of thallium emission myocardial tomography with 180° and 360° data collection. *J Nucl Med* 23:661–666, 1982
7. Tsui BMW, Gunter DL, Beck RN: Study of spatial resolution in SPECT. *J Nucl Med* 23:P45, 1982 (abstr)
8. Sorenson JA: Quantitative measurement of radioactivity in vivo by whole body counting. In *Instrumentation in Nuclear Medicine*, Vol 2, Hine GJ, Sorenson JA, eds. New York, Academic Press, 1974, p 311
9. McIntyre WJ, Go RJ, Houser TC, et al.: Evaluation of 180° and 360° reconstruction of the heart by transaxial tomography with thallium-201. In *Digital Imaging: Clinical Advances in Nuclear Medicine*, New York, The Society of Nuclear Medicine, 1982, pp 197–203
10. Go RJ, MacIntyre WJ, Hauser TS, et al: Clinical evaluation of 360° and 180° data sampling techniques for transaxial SPECT Thallium-201 myocardial perfusion imaging. *J Nucl Med* 26:695–706, 1985
11. Coleman RE, Jaszczak RJ, Cobb FR: Comparison of 180° and 360° data collection in thallium-201 imaging using SPECT. *J Nucl Med* 23:655–660, 1982
12. Shepp LA, Hilal SK, Schulz RA: The tuning fork artifact in computerized tomography. *Comput Tomogr Comput Graph Image Proc* 10:246–255, 1979
13. Pettigrew RI, Atwood E, Webb R, et al: SPECT compared to planar Tc-99m pyrophosphate infarct avid scintigraphy. *J Nucl Med* 24:P18, 1983 (abstr)
14. Nowak DJ, Eisner RL, Fajman W: Distance weighted backprojection: A SPECT reconstruction technique. *Radiology* 159:531–536, 1986
15. Ritchie JL, Williams DL, Harp G, et al: Transaxial tomography with thallium-201 for detecting remote myocardial infarction. *Am J Cardiol* 50:1236–1241, 1982
16. Garcia EV, VanTrain K, Maddahi J: Quantification of rotational thallium-201 myocardial tomography. *J Nucl Med* 26:17–26, 1985
17. Eisner RL, Gober A, Cerqueira M: Quantitative analysis of normal thallium-201 tomographic studies. *J Nucl Med* 26:P49, 1985 (abstr)